Glass transition, crystallization and thermoreversible gelation in ternary PPO solutions; relationship to asymmetric membrane formation

W. R. Burghardt, L. Yilmaz and A. J. McHugh
Department of Chemical Engineering, University of Illinois, Urbana, Illinois 61801, USA
(Received 29 December 1986; revised 20 April 1987; accepted 13 May 1987)

The phase equilibrium behaviour of PPO (poly 2,6-dimethyl-1,4-phenylene oxide) in mixtures of trichloroethylene with non-solvents ethanol, methanol or octanol has been studied. Attention has been given to the phenomena of glass transition, crystallization and thermoreversible gelation. The effect of solvent–non-solvent mixtures on the glass transition temperature depression was studied using differential scanning calorimetry (d.s.c.) and found to be well described by a ternary form of the Kelley–Bueche equation, using a modified best fit value of 3.67 for the solvent/polymer thermal expansivity ratio. Crystallization and gelation behaviour was studied using both d.s.c. and falling ball methods. D.s.c. scans showed a two-peaked behaviour when solvent trichloroethylene (TCE) or mixtures of TCE with octanol were used. Analysis showed that gel and crystal melting (associated with the higher temperature peak) are in a one-to-one correspondence and both exhibit a behaviour pattern with solvent concentration suggestive of simple melting point depression. However, addition of small amounts of non-solvent methanol or ethanol had a significant effect on the melting behaviour in that only a single endotherm resulted, whose depression in temperature could not be accurately described using the ternary form of the Flory melting point expression. A semi-quantitative discussion is given emphasizing the role of these phenomena in controlling both the nature of the ternary phase diagram and the structure formation processes associated with asymmetric membrane production.

(Keywords: PPO; membranes; glass transition; crystallization; gelation)

INTRODUCTION

Asymmetric membranes are generally prepared by phase inversion methods, the principal steps of which involve casting a thin film of a homogeneous polymer solution onto a suitable substrate, followed by quenching in a non-solvent bath. The non-solvent quench may be preceded by an evaporation period, but this is not necessary to obtain an asymmetric structure[1]. The principal structure-forming processes occur during the non-solvent quench, wherein solvent–non-solvent exchange occurs accompanied by the various phase transformations which lead to a given morphology. The development of quantitative models for the structuring process therefore requires an understanding of both the mass transfer and the thermodynamic characteristics of membrane-forming systems.

In a recent paper[2], Yilmaz and McHugh presented a systemization for the quantitative modelling of the quench period. Their approach involves calculating the complete ternary (non-solvent–solvent–polymer) phase diagram[3], followed by superposition of mass transfer paths based on a pseudo-binary diffusion formalism giving the locus of the ternary concentrations during the initial quench period. For systems in which liquid–liquid phase separation is the dominant process, such diagrams yield valuable insights into the nature of the conditions (i.e. non-solvent/solvent flux ratios, solvent densities, etc.) under which different skin structures might be expected. On the other hand, various authors have suggested that other types of phase separation may also play a role in the structure formation process. For example, Smolders and coworkers[4,5] have hypothesized that skin formation occurs during the rapid, initial stages of the quench in consequence of a gelation mechanism. The sublayer forms subsequently by liquid–liquid phase separation, followed by gelation in the concentrated phase which freezes in the porous, phase-separated morphology. Such gelation is believed to occur through a crystallization mechanism for crystallizable systems[4], or, in the case of amorphous polymers, by the system crossing some sort of viscosity boundary[5] at much higher polymer concentrations.

To develop complete ternary phase diagrams for use with mass transfer calculations, it would be desirable to represent gelation behaviour quantitatively. However, the issue of thermoreversible gelation is still open to some discussion with regard to both the relationship of crystallization and gel formation and its mechanism in amorphous systems[6–8]. For example, a number of authors have argued that gelation is a direct consequence of the formation of crystalline junctions and offer evidence in support of this view[9–13]. On the other hand, the definition of gelation and the so-called gel point has generally been based on rheologically defined phenomena (such as elasticity or rheopexy) and such response quite naturally suggests the likelihood of mechanical entanglement networks for its source rather than junction

0032-3861/87/122085-08$03.00

crystallization[14–18]. Some authors in fact emphatically state that crystallization is not an essential feature of gelation and that observations related to crystallinity, such as X-ray diffraction, have been due to polymer precipitation accompanying gelation rather than vice versa[19,20]. To date, only one study of gelation in a membrane-forming system has been reported, that being for ternary cellulose acetate systems[21]. Likewise, although the crystallization behaviour of cellulose acetate in ternary systems has been studied by differential scanning calorimetry (d.s.c.)[22,23], it has not been demonstrated that gelation does indeed result solely from crystallization. Thus it seems clear that construction of a gel region on a ternary phase diagram requires systematic analysis of both the gelation and the crystallization characteristics of a given membrane-forming system.

It is our belief that, for a number of reasons, an understanding of the glass transition behaviour of membrane-forming systems is also an essential aspect of the modelling of membrane formation. First, glass transition depression can provide a simple explanation for the hypothesized viscosity boundary mentioned earlier for non-crystallizable polymers. Second, as will be shown in this work, it provides an alternative explanation for skin formation and solidification of the porous sublayer in either crystallizable or amorphous systems. And, finally, since crystallization occurs very slowly relative to the millisecond time scale for skin formation[21,23], it is likely that such processes are kinetically excluded, thus leaving the glass transition as a logical source for dense skin formation[5,24]. For these reasons we have undertaken a study of the glass transition, thermoreversible gelation, and crystallization behaviour in the model system of PPO (poly 2,6-dimethyl-1,4-phenylene oxide) in mixtures of trichloroethylene with non-solvents ethanol, methanol or octanol. Our objective in this paper is to present a discussion of the resulting features of our study which have application to asymmetric membrane formation processes.

THEORY

Glass transition temperature depression

The phenomenon of glass transition temperature depression by low molecular weight diluents has received much attention due to its importance in plasticization. Theories which have been proposed to explain this behaviour can be broadly classified into those which treat the glass transition as a thermodynamic process and those which address its kinetic nature. We have found that the kinetic models based on free volume considerations provide the most straightforward explanation of the behaviour in our system[25].

The original equation based on free volume considerations was proposed by Kelley and Bueche[26] and is given as

$$T_g = \frac{R\phi_2 T_{g2} + \phi_3 T_{g3}}{R\phi_2 + \phi_3} \qquad (1)$$

where ϕ_i are the volume fractions of the diluent (2) and the polymer (3), T_{gi} are the pure component glass transition temperatures, and $R \equiv \alpha_2/\alpha_3$, with α_i being the difference in thermal expansivity between liquid and glass for component i. These values have generally been taken to be $\alpha_3 = 4.8 \times 10^{-4}$ and $\alpha_2 = 10^{-3}$, leading to the value[26] of $R = 2.1$. Modifications of equation (1) have been proposed with the object of obtaining better agreement with data using the 'universal' value of $R = 2.1$. The form given by Czekaj and Kapko[27] is

$$T_g = T_{g3} + R(T_{g2} - T_{g3})\phi_2 \qquad (2)$$

while that proposed by Chee[28] is

$$T_g = \frac{T_{g3} + (RT_{g2} - T_{g3})\phi_2 - R(R+1)(T_{g3} - T_{g2})\phi_2^2/4}{1 + (R-1)\phi_2} \qquad (3)$$

The Kelley–Bueche and Czekaj–Kapko equations can easily be generalized to ternary forms useful for describing non-solvent–solvent–polymer systems. In such a case, for mixtures of two diluents, 1 and 2, one obtains the following expressions for these two models.

$$T_g = \frac{R_1\phi_1 T_{g1} + R_2\phi_2 T_{g2} + \phi_3 T_{g3}}{R_1\phi_1 + R_2\phi_2 + \phi_3} \qquad (4)$$

and

$$T_g = T_{g3} + R_1(T_{g1} - T_{g3})\phi_1 + R_2(T_{g2} - T_{g3})\phi_2 \qquad (5)$$

where $R_i = \alpha_i/\alpha_3$. These can easily be solved to generate a curve on the ternary phase diagram for which T_g has a given desired value (e.g. room temperature).

Crystal melting point depression

When low molecular weight solvents do not enter the polymer crystal lattice, their effect on the equilibrium melting point results solely from the change in the free energy of mixing of the solution, which can be well described by classical Flory–Huggins solution theory for the binary polymer–solvent system. The equilibrium state between a perfect crystal and a ternary solution may likewise be described using the appropriate ternary form of Flory–Huggins[29]. Starting from the extended form for the Gibbs energy of mixing with concentration-dependent interaction parameters[3], g_{ij},

$$\begin{aligned}\frac{\Delta G_m}{RT} &= n_1 \ln\phi_1 + n_2 \ln\phi_2 + n_3 \ln\phi_3 + g_{12}(u_2) n_1 \phi_2 \\ &\quad + g_{13}(\phi_3) n_1 \phi_3 + g_{23}(\phi_3) n_2 \phi_3\end{aligned} \qquad (6)$$

where the n_i are moles of component i and $u_2 = \phi_2/(\phi_1 + \phi_2)$, one can readily derive the following ternary form for the melting point depression equation:

$$\begin{aligned}\frac{1}{T_m} - \frac{1}{T_m^\circ} = -\frac{R}{\Delta H_f^\circ}\Bigg\{ &\ln\phi_3 + (1-\phi_3) - \frac{v_3}{v_1}\phi_1 - \frac{v_3}{v_2}\phi_2 \\ &+ \left(g_{13}\frac{v_3}{v_1}\phi_1 + g_{23}\frac{v_3}{v_2}\phi_2\right)(\phi_1 + \phi_2) - g_{12}\frac{v_3}{v_1}\phi_1\phi_2 \\ &+ \left[\frac{v_3}{v_1}\phi_1\left(\frac{dg_{13}}{d\phi_3}\right) + \frac{v_3}{v_2}\phi_2\left(\frac{dg_{23}}{d\phi_3}\right)\right]\phi_3(\phi_1 + \phi_2)\Bigg\}\end{aligned} \qquad (7)$$

In equation (7), T_m is the crystal melting point in the presence of the non-solvent–solvent mixture, T_m° is the pure crystal melting point, ΔH_f° is the equilibrium heat of fusion and the v_i are molar volumes of the respective species. Hence, given a knowledge of these parameters, along with concentration dependencies of the g_{ij}, one can construct a curve on the ternary phase diagram representing a given fixed value for T_m.

EXPERIMENTAL

Materials

The PPO resin used (supplied by General Electric) was characterized by a number average molecular weight of 25000. A d.s.c. trace of the pure powder was found to exhibit a melting endotherm from 235 to 265°C. Following a rapid quench and upon reheating, the same sample exhibited a discontinuity in heat capacity indicative of a glass transition at 211°C in excellent agreement with previously published results[30]. All chemicals (trichloroethylene (TCE), methanol, chloroform, toluene and octanol) were used as received. Pure component glass transition temperatures for the diluents were taken from the literature: TCE, 107 K [31]; toluene, 113 K [32]; methanol, 103 K [33]; ethanol, 97 K [31] and n-octanol, 145 K [31] *.

Apparatus

D.s.c. measurements were made using two calorimeters. Glass transition experiments were carried out on a Perkin–Elmer DSC-4 interfaced with a System 7/4 thermal analysis controller and a model 3600 thermal analysis data station. Crystallization experiments were carried out on a DuPont 910 DSC interfaced with a 1090 thermal analyser. Both instruments were equipped with cooling accessories for sub-ambient operation. Temperature standards used for calibration were indium ($T_m = 156.6$°C), n-decane ($T_m = -29.66$°C) and *p*-nitrotoluene ($T_m = 51.64$°C). The heat flow axis of the Perkin–Elmer calorimeter was calibrated using an internally generated electronic signal, while the heat of fusion of the indium sample was used to calibrate the DuPont instrument. All samples were contained in volatile-sample pans, which were sealed using a specially designed crimping tool.

Gelation experiments were carried out in a glass tube designed to minimize vapour space, due to the differences in volatility among the solvent and non-solvents used[25]. Temperature was maintained in a variety of thermostated oil baths, and gel melting temperatures were determined using the 'falling ball' method, with a $\frac{1}{16}$in (1.6 mm) steel ball. Ball height was monitored using a cathetometer having an accuracy of 0.005 cm.

Glass transition measurements

Samples were prepared following one of two procedures. For PPO in TCE or toluene, concentrated samples were made by evaporating the solvent from homogenous solutions for various amounts of time. Pieces of the resultant rigid material were weighted into d.s.c. sample pans, which were then sealed. For ethanol or methanol as the diluent, samples were prepared by soaking films of amorphous PPO in the alcohol for various amounts of time, after which the films were dried with a tissue, and pieces weighed into the sample pans. In either case, the exact composition of the samples was determined subsequent to the thermal analysis, by puncturing the pan, heating under vacuum for one day at a temperature above the boiling point of the diluent, and weighing to determine the weight loss.

Glass transition temperatures were measured by observation of the characteristic discontinuity in the d.s.c. trace. Samples obtained by concentration from homogeneous solution were first heated well above the glass transition temperature to destroy any crystalline structure which may have formed during evaporation of the solvent. After a rapid temperature quench, the d.s.c. trace was taken at a heating rate of 10°C min^{-1}. For samples of PPO in alcohols, since the initial polymer film was amorphous, the d.s.c. trace could be taken immediately, again heating at 10°C min^{-1}. Such traces generally exhibited broadened transitions, due possibly to inhomogeneity of the samples, and/or the low boiling point of the alcohol diluent.

Crystallization

Samples for crystallization experiments were prepared by weighing the appropriate amount of PPO powder and solvent (or solvent/non-solvent mixture) directly into the d.s.c. sample pans. Homogeneous solutions were prepared by heating the sealed pans above the melting point for at least one day, followed by various cooling programmes to induce crystallization under a variety of thermal histories. Samples were then heated at a rate of 10°C min^{-1} to observe the melting endotherms of the crystals formed during the cooling steps.

Gelation experiments

Appropriate amounts of PPO powder and solvent (or solvent/non-solvent mixture) were weighed into the gelation tube, which was then sealed with the ball in the tube. The tube was then placed in an oil bath and heated to form a homogeneous solution. After 24 h, the ball was suspended in the solution with a magnet and the tube and magnet were then transferred to a bath held at 25°C, whereupon gels were formed for 36 h.

The prepared gels were then placed in a third oil bath, held at 25°C, which was then heated at a rate of 0.5°C min^{-1} while the ball height was recorded as a function of bath temperature.

RESULTS

Glass transition

Data for the PPO glass transition temperature are shown in *Figure 1* along with predictions based on the free volume theories (equations (1)–(3)). Although both the Czekaj–Kapko and Chee models provide an improved fit over the Kelley–Bueche equation, none of the three adequately describes the observed behaviour using the universal value of $R = 2.1$. On the other hand, treating R as an adjustable parameter allows a better fit to the data. Using this approach for all three equations led to the best fit with equation (1) for a value of $R = 3.67$, shown as the solid line in *Figure 1*. To exclude the possibility that specific molecular interactions, such as hydrogen bonding between TCE and the ether linkage in PPO, might be responsible for the higher R value, experiments were also carried out with the system PPO/toluene. The results are presented in *Figure 2*, where again the solid line has been calculated from equation (1) using the value of $R = 3.67$.

---

* Estimated from published data on n-alcohols

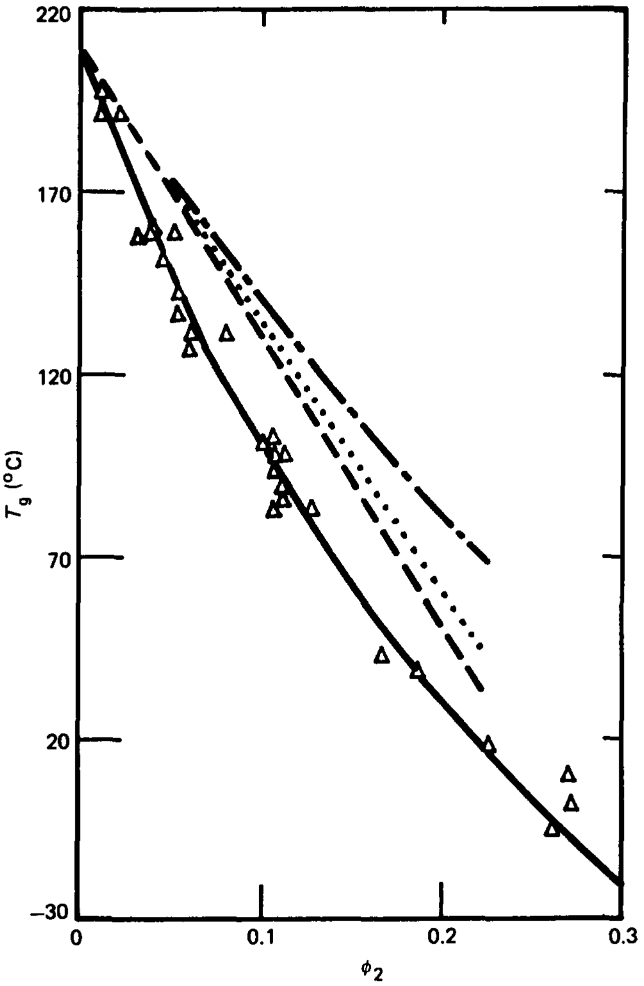

Figure 1 Glass transition temperature against volume fraction TCE. Lines drawn for $R=2.1$: (–·–·–), equation (1); (– – –), equation (2); (·····), equation (3); and $R=3.67$ (———), equation (1)

Since an equally good fit results for both toluene and TCE, one can conclude that the high value of R is not due to specific TCE–PPO interactions.

To rationalize the value of 3.67, it is useful to recall the definition of R as a ratio of thermal expansivity differences between subcooled liquids and glasses. It has generally been assumed that the same values of α_2 and α_3 adequately describe the behaviour of all diluents and polymers, respectively. However, wide variations exist in thermal expansivities of polymers[33]. In addition, since the bulk expansivity of PPO is extremely low compared to other polymers, it is not unreasonable to expect that α_3 would likewise be lower than that observed for other systems. Since expansivities of low molecular weight diluents generally exhibit much less variation, we conclude that the high R is due primarily to a lower value of α_3. It is interesting to note that there has been a general reluctance in the literature to treat R as an adjustable parameter. In fact, the tendency has been more to change the equation in order to fit data than to change this parameter[27,28]. However, given the wide range of properties possible in polymeric systems, we believe that our empirical fit is a more reasonable approach for the interpretation of data.

Results for the glass transition depression with non-solvent ethanol are shown in *Figure 3*, along with the predictions of equation (1), again using the value $R=3.67$. Despite the extreme differences in quality between solvent and non-solvent, this value still provides a good fit to the data. Experiments with methanol were complicated due to its high volatility[25]. However, the results shown here indicate that the same value of R may be used for T_g depression of both solvent and non-solvent.

Using the best fit value for R, equation (4) can be solved to generate the locus of compositions for which $T_g=25$°C. The results of such a calculation are shown in *Figure 4* for the system ethanol/TCE/PPO. The liquid binodal and spinodal curves shown were generated using the algorithm discussed by Yilmaz and McHugh[3]. The non-solvent polymer interaction parameter, g_{13}, was evaluated experimentally using the method described by Mulder and Smolders[34]. Vapour–liquid equilibrium data from the literature[35] were used to generate a quadratic expression for g_{12}, and g_{23} was determined from a least squares analysis of our crystal melting point data.

The most informative aspect of this diagram relates to the fact that a portion of the concentrated branch of the binodal curve passes into the glassy region. Thus, during quenching, as solvent diffuses out of the cast film, the equilibrium concentrated phase should eventually become a glass, thus providing a simple mechanism for solidification of the porous phase-separated structure. It has previously been argued that gelation, induced by crystallization, is responsible for sublayer soldification[4]. However, this interpretation is inconsistent with the observation that formed PPO membranes exhibit little or no d.s.c. melting endotherm, a point which is however entirely consistent with the occurrence of glass formation.

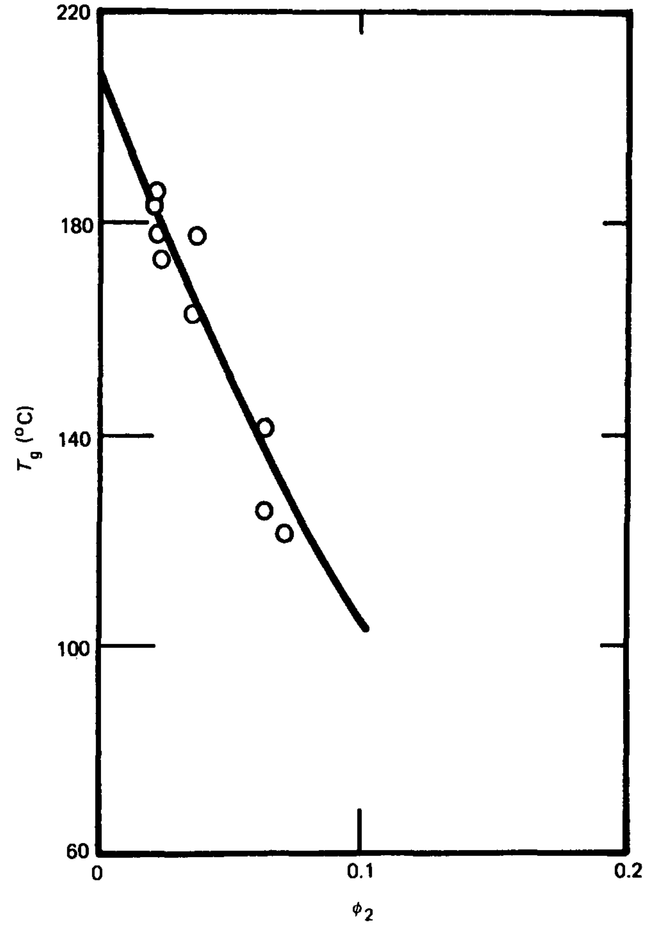

Figure 2 Glass transition temperature against volume fraction toluene. Solid line, equation (1) with $R=3.67$

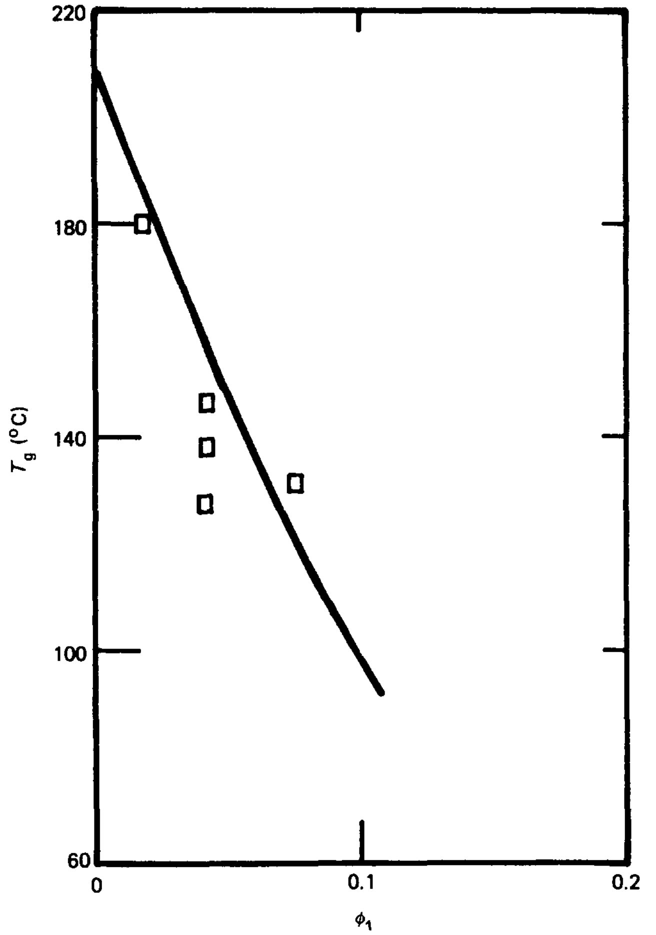

Figure 3 Glass transition temperature against volume fraction ethanol. Solid line, equation (1) with $R=3.67$

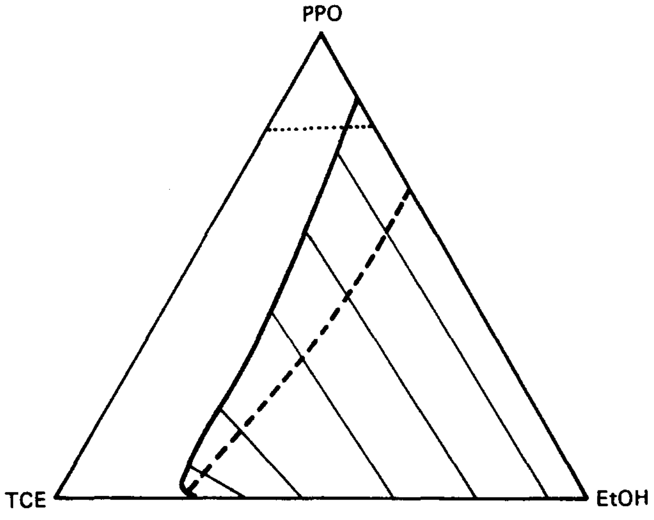

Figure 4 Glassy region boundary (·····) superimposed on liquid–liquid phase diagram for ethanol/TCE/PPO system at 25°C. Parameters: $R_1=R_2=3.67$, $g_{12}=1.31-0.32u_2+1.30u_2^2$, $g_{13}=1.48$, $g_{23}=0.215$, $v_3/v_2=260$, $v_3/v_1=400$

One also finds that the glassy region boundary in *Figure 4* is very near the arbitrarily plotted 'viscosity boundary' proposed for the amorphous polysulphone system[5]. If instead of $T_g=25°C$, one were to use the value of 0°C, corresponding to an ice bath quench condition, the glass transition curve would shift downward, (approximately 5–6% decrease in ϕ_3), thus further expanding the glassy region associated with the concentrated liquid portion of the binodal. Thus it seems likely that, in the absence of crystallization, dense-skinned membranes may result from a glass transition during the skin formation step. Likewise, for the PPO system, it seems likely that diffusion during skin formation should be rapid enough for the same glass formation mechanism to hold, such as in the case of dense-skinned PPO pervaporation membranes. To justify such a conclusion, however, it is necessary to evaluate the gelation/crystallization behaviour of this system.

Crystallization

Figure 5 shows the results of a set of d.s.c. experiments run on a sample of PPO in pure TCE. The homogeneous solution was cooled from 135 to 35°C at 10°C min^{-1} and held at this temperature for various amounts of time, followed by continued cooling to -5°C. After 2 min, the sample was reheated to 135°C at 10°C min^{-1}, resulting in the given thermograms. Two distinct peaks are observed, with their relative sizes determined by the time spent at 35°C. When no time is allowed, the lower-melting peak dominates, while as more time is allowed, the higher-melting peak increases in size as the lower peak disappears. Reducing the cooling rate from 10°C min^{-1} to 1°C min^{-1} has the same effect as waiting at 35°C, i.e. the second peak grows at the expense of the first. A similar double-peaked behaviour has been observed in earlier studies on solutions of PPO in decalin[36] and toluene[37] and, in both cases, the higher temperature peak has been observed to grow at the expense of the lower one. It was concluded that the two peaks reflect different crystal forms, with the lower melting peak representing a faster growing metastable form which preferentially results when the sample is cooled sufficiently quickly[37]. We believe this interpretation applies to the present case as well.

Addition of small amounts of octanol had no significant effect on the two-peaked behaviour or melting temperature. However, addition of small amounts of either methanol or ethanol to the solvent produced a dramatically different pattern in the resultant thermograms. *Figure 6* shows the results of a set of d.s.c. experiments on a solution of PPO dissolved in a mixture of TCE and ethanol. Quench procedures were similar to

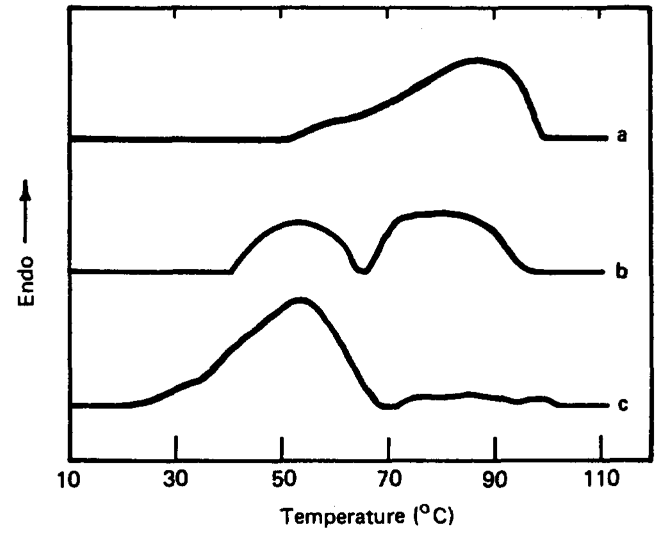

Figure 5 D.s.c. thermograms of a solution of PPO in TCE ($\phi_3=0.486$) taken at a heating rate of 10°C min^{-1} after holding at various times at 35°C during cooling: (a) 10 min; (b) 5 min; (c) 0 min

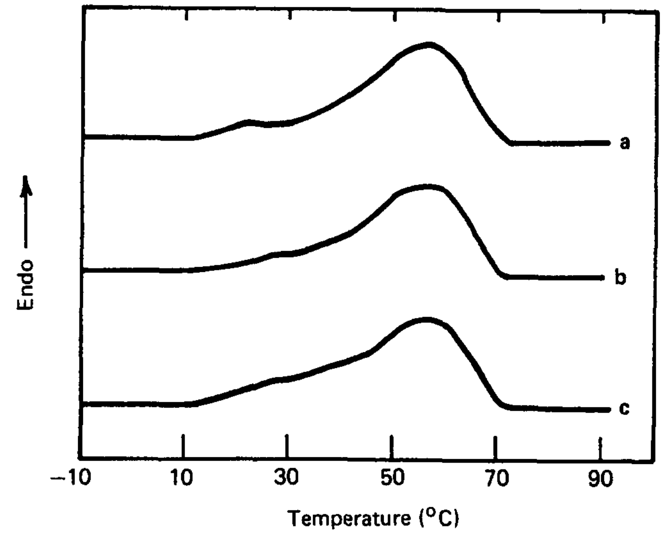

Figure 6 D.s.c. thermograms of a solution of PPO in TCE/ethanol (98:02) ($\phi_3 = 0.467$) after holding at various times at 20°C during cooling: (a) 10 min; (b) 5 min; (c) 0 min

those used with pure TCE and were carried out over the range −40°C to 110°C, allowing various holding times at 20°C. One sees that the melting behaviour for this system is considerably different in that only a single endotherm is observed, which is basically unaffected by the cooling pattern. Also, varying the cooling rate between 80°C min^{-1} and 1°C min^{-1} produced no discernible effect on the peak location. In addition to the substantial qualitative changes, one also finds that the melting temperature is strongly depressed by the presence of the ethanol. Experiments using alcohol concentrations as high as 11% led to similar results and experiments with methanol gave essentially the same results as those shown here for the ethanol[25].

Gelation behaviour

Gelation experiments were carried out using a wide variety of solvent/non-solvent combinations and concentrations. In all cases the gels which formed were turbid, with the turbidity gradually disappearing on heating and finally clearing near the gel melting temperature. For the systems which were also studied calorimetrically, comparisons can be made between the crystal and gel melting points. A collection of such data is shown in *Figure 7*. Crystal melting points were taken as the temperature where the d.s.c. endotherm returned to the baseline, since this corresponds to the complete disappearance of the crystallinity. For pure TCE and TCE/octanol the higher melting endotherm was used. As is evident from the data on these four systems, a clear correlation exists between gel and crystal melting. The important conclusion can therefore be made that, in this region of the phase diagram, gelation corresponds to crystallization. This conclusion is entirely consistent with the appearance of the gels during melting: the gradual decrease in turbidity corresponds to the wide endothermic peak in the d.s.c. traces and the final disappearance of turbidity is caused by the melting of the last crystals in the system which maintain the three-dimensional gel network.

If gelation results from a crystallization process, it should be possible to analyse these data in terms of the Flory melting point expression (equation (7)). *Figure 8* shows the results of such an analysis for the system PPO/TCE/ethanol for various solvent compositions, along with predictions based on equation (7). Expressions for the liquid interaction parameters used in the calculations were those in the caption of *Figure 4*. The value used for ΔH_f° was 47.7 J g^{-1}, as determined by a fit of our binary PPO/TCE melting point data[25]. Since gel melting correlates with the d.s.c. end point, the equilibrium melting temperature of the pure PPO powder was likewise evaluated and found to be 260°C. One clearly sees from *Figure 8* that the crystal melting point expression cannot explain the extreme depression in T_m which occurs with the addition of small amounts of the non-solvent. Since the crystallization behaviour of PPO is known to depend strongly on the solvent medium with the possibility that diluent molecules may be incorporated in the crystal lattice, it is not unlikely that small amounts of non-solvent, such as ethanol or

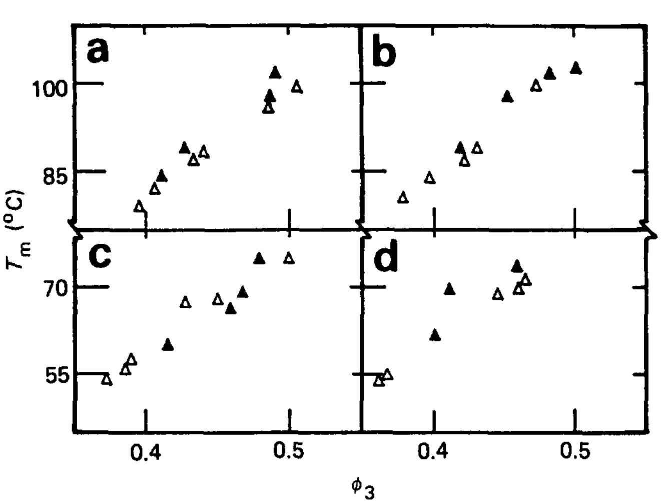

Figure 7 Gel/crystal melting point from falling ball (△) and d.s.c. (▲) experiments for solutions of PPO in: (a) pure TCE; (b) TCE/octanol (98:05); (c) TCE/ethanol (98:02); (d) TCE/methanol (95:05)

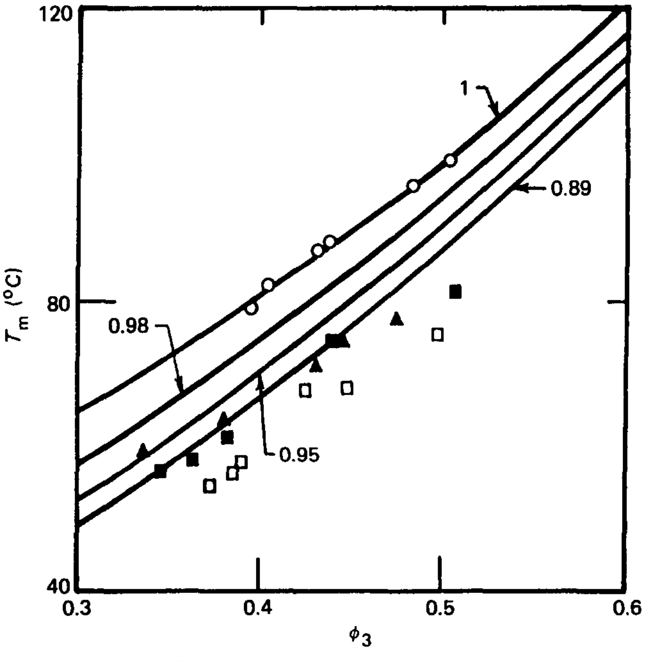

Figure 8 Gel melting temperature against volume fraction PPO for solutions in TCE/ethanol: 100:0 (○); 98:02 (□); 95:05 (■); 89:11 (▲). Solid lines predicted by equation (7) for indicated u_2

methanol, could have a strong effect on the lattice structure. This would necessitate modification of the chemical potential expression for the crystal phase in the Flory melting point analysis, which in turn would affect both the melting temperature and the heat of fusion. In addition, the use of equation (7) implicitly assumes one is dealing with an equilibrium crystal state, whereas it is a well known fact that polymer crystallization is a highly non-equilibrium process[38]. Thus, although we believe our data clearly show that gelation in PPO most likely corresponds to a crystallization mechanism, quantitative analysis must await a more complete understanding of both the thermodynamics and kinetics of this process.

DISCUSSION

Although the Flory equation does not provide an accurate quantitative description of PPO melting point depression in the presence of non-solvent, it does nonetheless offer a useful basis for analysing the relative effects of crystallization on the ternary phase diagram. Determination of the phase diagram requires numerical solution of equation (7) for a specific temperature (25°C) in conjunction with calculation of the ternary binodal curve[3]. The results of such phase diagram calculations, based on parameters for the PPO/TCE/ethanol system, are presented in *Figure 9*. The saturation curve, consisting of tie lines connecting the pure equilibrium crystal with a given liquid composition, proceeds from the polymer–solvent axis to the point of intersection with the liquid binodal curve. The liquid tie line at this point also connects with another liquid phase, thereby creating an equilibrium three-phase region. Once the saturation curve emerges from the dilute end of this tie line, crystallization again becomes the thermodynamically preferred state across the remainder of the phase diagram.

The behaviour pattern exhibited in *Figure 9* is typical of a crystallizable system and such a phase diagram offers a basis for further insight into the membrane formation process. The most important conclusion one reaches is that crystallization is the thermodynamically preferred phase transition over most of the phase diagram. As mentioned earlier, however, PPO membranes generally exhibit little or no d.s.c. melting endotherm. Therefore we conclude that, during membrane formation, metastable liquid phase boundaries control the phase separation process, with the resultant concentrated liquid phase being too viscous to allow crystal nucleation and growth before vitrification takes place. Hence, as far as sublayer solidification is concerned, kinetic factors outweigh the thermodynamics.

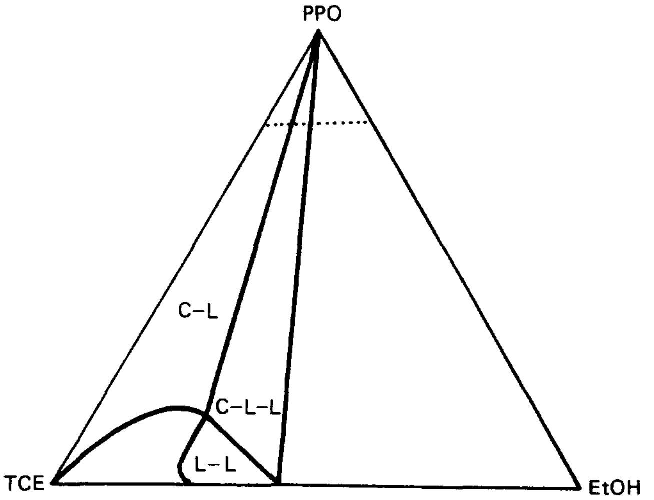

Figure 9 Equilibrium phase diagram at 25°C for ethanol/TCE/PPO, showing crystal–liquid (C–L), liquid–liquid (L–L) and crystal–liquid–liquid regions (C–L–L). Glassy region boundary also shown

Another area of interest in the crystal–liquid phase diagram corresponds to the region near the polymer–solvent axis where gelation has been suggested to be the mechanism for skin formation. For example, in the preparation of PPO ultrafiltration membranes it has been found that the addition of small amounts of non-solvent octanol to the recipe promotes the formation of structures having a microporous skin[4,39]. It was hypothesized that the presence of octanol affects crystallization during gelation in such a way as to induce pore growth during the skin formation[39]. On the other hand, our results indicate that octanol has a negligible qualitative (two-peaked) as well as quantitative (melting temperature) effect on the gelation/crystallization behaviour. Furthermore, it has been shown[4] that the presence of octanol has no major effect on the kinetics of the crystallization process in this region of the phase diagram. Likewise, model quanternary calculations indicate that introduction of octanol into the system has only a small effect on the location of the glass region boundary[25]. On the other hand, the addition of octanol does cause a significant shifting of the liquid phase diagram, bringing the system much closer to a phase separated condition[4,25]. Thus we conclude that in order to obtain microporous skins in ultrafiltration membranes it is necessary for the coagulation path to enter the liquid two-phase region during quenching. Based on time scale considerations, therefore, spinodal decomposition followed by vitrification becomes a real possibility for skin formation. A similar conclusion may also be drawn from published results on polysulphone in which the initial concentration has been varied[5].

The origin of dense skin formation in membranes of crystallizable polymers such as PPO or cellulose acetate is more difficult to determine[24]. It is not possible to determine whether solidification of a dense top layer is to be attributed to either a gelation or a glass transition effect by simply analysing the formed membrane. However, since it has been noted that skin formation probably occurs on a millisecond time scale[21,23], for reasons mentioned earlier, glass transition effects would be of importance in dense skin formation in these systems as well. In our current studies we are investigating different non-crystalline polymers such as polyimides and polysulphones in order to develop a data base for comparing crystallizable and non-crystallizable membrane-forming systems.

In summary, we believe the results of our study clearly show that the processes of gelation and crystallization in PPO are highly related. However, the time scales are too large for such a process to be a causative mechanism in skin formation. On the other hand, glass transition offers a qualitative and quantitative mechanism for freezing in the phase-separated structures which result in the initial quench period and is consistent with both the thermodynamic and mass transfer aspects of membrane structure formation.

REFERENCES

1 Sarbolouki, M. N. *J. Polym. Sci., Polym. Lett. Edn.* 1973, **11**, 753
2 Yilmaz, L. and McHugh, A. J. *J. Membrane Sci.* 1986, **28**, 287
3 Yilmaz, L. and McHugh, A. J. *J. Appl. Polym. Sci.* 1986, **31**, 997
4 Wijmans, J. G., Rutten, H. J. J. and Smolders, C. A. *J. Polym. Sci., Polym. Phys. Edn.* 1985, **23**, 1941
5 Wijmans, J. G., Kant, J., Mulder, M. H. V. and Smolders, C. A. *Polymer* 1985, **26**, 1539
6 Tan, H. M., Chang, B. H., Baer, E. and Hiltner, A. *Eur. Polym. J.* 1983, **19**, 1021
7 Gan, J. Y. S., Francois, J. and Guenet, J.-M. *Macromolecules* 1986, **19**, 173
8 Domszy, R. C., Alamo, R., Edwards, C. O. and Mandelkern, L. *Macromolecules* 1986, **19**, 310
9 Takahashi, A., Nakamura, T. and Kagawa, I. *Polym. J.* 1972, **3**, 207
10 Girolamo, M., Keller, A., Miyasaka, K. and Overbergh, N. *J. Polym. Sci., Polym. Phys. Edn.* 1976, **14**, 39
11 Various papers in 'Gels and gelling processes', *Faraday Discuss. Chem. Soc.* 1974, **57**
12 Takahashi, A. *Polym. J.* 1973, **4**, 379
13 Bisschops, J. *J. Polym. Sci.* 1954, **12**, 583; 1955, **17**, 89
14 Layec-Raphalen, M. N. and Wolff, C. J. *Non-Newtonian Fluid Mech.* 1976, **1**, 159
15 Wolff, C., Silberberg, A., Priel, Z. and Layec-Raphalen, M. N. *Polymer* 1979, **20**, 281
16 Wolff, C. *Adv. Colloid Interface Sci.* 1982, **17**, 263
17 Edwards, S. F. *Faraday Discuss. Chem. Soc.* 1974, **57**, 47
18 Kraemer, E. O. and Faneslow, J. R. *J. Phys. Chem.* 1925, **29**, 1169
19 Labudzinska, A., Wasiak, A. and Ziabicki, A. *J. Polym. Sci. C* 1967, **16**, 2835
20 Labudzinska, A. and Ziabicki, A. *Kolloid Z. Z. Polym.* 1971, **243**, 21
21 Reuvers, A. J., Altena, F. W. and Smolders, C. A. *J. Polym. Sci., Polym. Phys. Edn.* 1986, **24**, 793
22 Altena, F. W. and Smolders, C. A. *J. Polym. Sci., Polym. Phys. Edn.* 1981, **69**, 1
23 Altena, F. W., Schroder, J. S., Van de Huls, R. and Smolders, C. A. *J. Polym. Sci., Polym. Phys. Edn.* 1986, **24**, 1725
24 Mulder, M. H. V., Hendrikman, J. O., Wijmans, J. G. and Smolders, C. A. *J. Appl. Polym. Sci.* 1985, **30**, 3805
25 Burghardt, W. R. *M.S. Thesis*, Univ. of Illinois, Urbana, Illinois, 1986
26 Kelley, F. N. and Bueche, F. *J. Polym. Sci.* 1961, **50**, 549
27 Czekaj, T. and Kapko, J. *Eur. Polym. J.* 1981, **17**, 1227
28 Chee, K. K. *Eur. Polym. J.* 1985, **21**, 29
29 Flory, P. J. 'Principles of Polymer Chemistry', Cornell University Press, Ithaca, 1953
30 Karasz, C. E. and O'Reilly, J. M. *J. Polym. Sci., Polym. Lett. Edn.* 1965, **3**, 561
31 Lesikar, A. V. *J. Chem. Phys.* 1975, **63**, 2297
32 Privalko, V. *J. Phys. Chem.* 1980, **84**, 3307
33 Mark, H. E. (Ed.) 'Encyclopedia of Polymer Science and Technology', John Wiley, New York, 1973, Vol. 13, p. 780
34 Mulder, M. H. V. and Smolders, C. A. *J. Membrane Sci.* 1984, **17**, 289
35 Gmehling, J. and Onken, O. (Eds.) 'Vapour–liquid Equilibrium Data Collection', Vol. 2A, Friedrich Bischoff, Frankfurt, 1977
36 Janeczek, H., Turska, E., Szekely, T., Lengyel, M. and Till, F. *Polymer* 1978, **19**, 85
37 Koenhen, D. M. and Smolders, C. A. *J. Polym. Sci., Polym. Phys. Edn.* 1977, **15**, 167
38 Wunderlich, B. 'Macromolecular Physics', Academic Press, New York, 1976, Vol. 2
39 Broens, L., Loenhen, D. M. and Smolders, C. A. *Desalination* 1977, **22**, 205